

A Study of the Equilibrium and Kinetics of Urea Binding by a Biomimetic Dinickel(II) Complex

Sergey V. Kryatov,^[a] Elena V. Rybak-Akimova,^{*[a]} Franc Meyer,^{*[b]} and Hans Pritzkow^[c]

Dedicated to Professor George M. Sheldrick on the occasion of his 60th birthday

Keywords: Enzyme models / Nickel / N ligands / Kinetics / Thermodynamics

The equilibrium and kinetics of urea binding by model dinickel complexes have been studied, which is relevant to the activity of the urease enzyme. The pyrazolate-based, O₂H₃-bridged dinuclear nickel(II) complex [LNi₂(OH)(H₂O)]²⁺ (**1**) binds urea reversibly in organic solvents with the formation of an N,O-bridged urea anion complex [LNi₂[OC(NH₂)NH]]²⁺ (**2**) and two water molecules. The equilibrium constant has been measured as 4.3(4) in acetone, 2.7(5) in acetonitrile, and 3(1) in methanol at 25 °C. Upon dissolving **1** in anhydrous methanol, the O₂H₃ bridge is substituted for an O₂Me₂H bridge to give [LNi₂(OMe)(MeOH)]²⁺ (**4**), which has been crystallized as **4**·(ClO₄)₂ and characterized by X-ray diffraction. Both Ni^{II} ions in **4** are five-coordinate with geometries intermediate between square-pyramidal and trigonal-bipyramidal. The H atom in the Me₂O₂H bridging unit is located in an asymmetric position. The exchange of water and methanol ligands in complexes **1** and **4** is very fast in solution at 25 °C (*k*_{obsd.} > 10³ s⁻¹). Binding of urea by complexes **1** and **4** are slower reactions (*k*_{obsd.} ≈ 10⁻¹ to 10¹ s⁻¹ under the concentration conditions used) and can be monitored by stopped-flow techniques. Detailed kinetic

studies indicate that binding of urea is a multi-step process. Steady-state intermediates of the tentative formula [LNi₂(OR)(urea)_{*n*}]²⁺ (*n* = 1, 2) are formed in fast preequilibrium with the starting complexes **1** (R = H) and **4** (H = Me), respectively. The bidentate N,O-coordination and deprotonation of an O-bound urea ligand constitute the overall rate-limiting step. The kinetic data suggest that both mono- and bis(urea) complexes participate in the formation of the chelate **2**, and that the latter are substantially more reactive. The bis(urea) pathway was unexpected because only one urea molecule is incorporated into the final product **2**. Reactive intermediates [LNi₂(OH)(urea)_{*n*}]²⁺ are close analogs of the reactive intermediate of urease, which also has the hydroxide and urea ligands bound at a dinickel core. However, the reactivities of the intermediates are different. The hydroxide ligand in our model complex acts as a base towards urea, and the urea anion complex **2** is formed. In urease, the hydroxide ligand attacks urea as a nucleophile leading to the hydrolysis of urea.

(© Wiley-VCH Verlag GmbH & Co. KGaA, 69451 Weinheim, Germany, 2003)

Introduction

Urease is an exceptional metallohydrolase that is present in various plants, fungi and bacteria. It contains two proximate nickel ions within its active site and efficiently catalyzes the hydrolysis of urea to finally give carbon dioxide and 2 equiv. of ammonia.^[1,2] This is a very remarkable reaction because urea has a very high resonance energy and hence is an extremely stable molecule. In fact, the uncata-

lyzed hydrolysis of urea has never been observed, while in aqueous solution urea slowly decomposes by an elimination pathway to yield ammonium cyanate.^[3] Since the first X-ray crystal structure of microbial urease was published in 1995,^[4] accumulating crystallographic evidence has provided a detailed picture of the enzyme active site and a reliable background for understanding its mechanism of catalysis.^[5–7] Based on the crystal structures of urease inhibited by either phosphate or diamidophosphate, as well as on the basis of recent model calculations and the mechanistic studies of enzyme inhibition, the process outlined in Scheme 1 now seems most probable.^[7,8] It implies that urea first coordinates to one nickel ion through its carbonyl oxygen atom, followed by a transition towards a bridging binding mode and concomitant nucleophilic attack by the bridging hydroxide ligand. The exact sequence of the latter events remains unclear, but work on synthetic model compounds suggests that urea becomes quite acidic (down to p*K*_a = 3 in aqueous solution) and tends to deprotonate upon N-

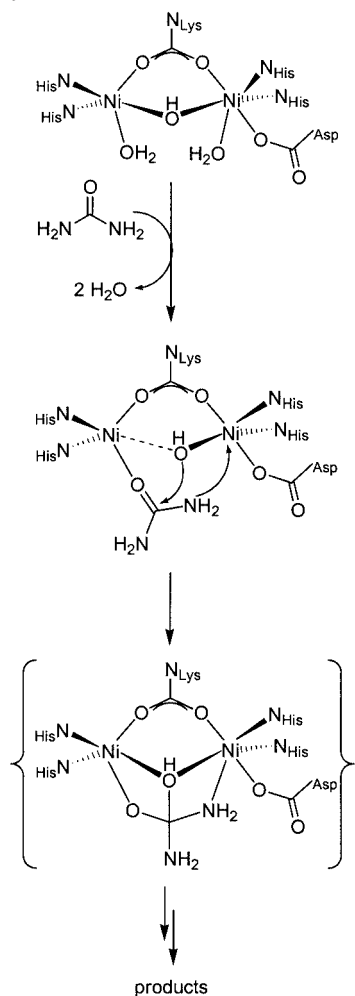
^[a] Department of Chemistry, Tufts University, Medford, Massachusetts 02155, USA
Fax: (internat.) + 1-617/627-3443
E-mail: elena.rybak-akimova@tufts.edu

^[b] Institut für Anorganische Chemie, Georg-August-Universität, Tammannstrasse 4, 37077 Göttingen, Germany
Fax: (internat.) + 49-551/393063
E-mail: franc.meyer@chemie.uni-goettingen.de

^[c] Anorganisch-Chemisches Institut der Universität Heidelberg
Im Neuenheimer Feld 270, 69120 Heidelberg, Germany

Supporting information for this article is available on the WWW under <http://www.eurjic.org> or from the author.

coordination.^[9] This should be even more pronounced upon bidentate *N,O*-binding to two metal ions, thereby rendering the substrate more resistant to hydrolysis under the optimal pH conditions of urease (pH = 4–8).^[10] It thus seems likely that one of the Ni–OH bonds is weakened upon initial binding of the substrate, and that formation of the bridging Ni–N_{urea} bond and nucleophilic attack occur simultaneously.^[7,8,11]

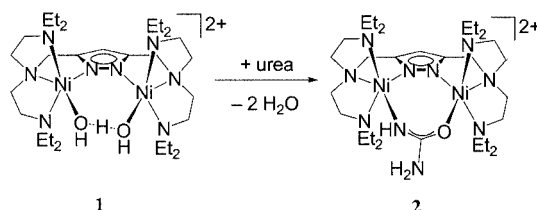


Scheme 1

Several synthetic dinickel model complexes have been prepared to mimic structural or functional features of the urease active site.^[11–16] In most model systems where urea coordination has been structurally verified, the substrate is bound through its carbonyl O atom, which is the preferred urea binding mode.^[14] In the very few systems showing a dinickel site with a bidentate *N,O*-bridging urea,^[11,15,16] the substrate is deprotonated as a ureate anion. Clearly, elucidation of the details of substrate binding is a prerequisite for a comprehensive understanding of urease activity. Likewise, control of urea binding in dinickel model complexes is crucial for achieving urease-like reactivity.

We have therefore carried out an in-depth analysis of the equilibrium and kinetics of urea binding by the active dinickel compound **1**, which was shown to give ureate-

bridged **2** in an acid/base reaction according to Scheme 2.^[15] The bridging pyrazolate in **1** and **2** was anticipated to most closely resemble the bridging carboxylate of the native enzyme (i.e. a carboxylated lysine residue), since both bridging units are monoanionic and can support similar metal–metal distances (from 3.3 to 4.6 Å for pyrazolate-bridged complexes).^[11,12e,13,14d,15,16,17,19,20] Short pendant arms (such as in complex **1**) enforce larger M–M separations. Complex **1** was chosen to specifically investigate the reactivity of an Ni-bound hydroxide ligand that can not bridge the two Ni centers. In urease, both terminal and bridging hydroxide ligands are present. Complex **1** possesses an intramolecular O₂H₃ bridge that can be described as a hydrated form of an active Ni-bound hydroxide ligand. This terminal hydroxide ligand is expected to be much more reactive as a base compared with a bridging hydroxide ligand. The latter is prevented in **1** due to the large Ni...Ni separation (4.5 Å, as compared to 3.5 Å in urease) enforced by the compartmental pyrazolate ligand scaffold.^[13,17] Urea incorporation by the diiron(III) complex [Fe₂(tpa)₂(μ-O)(O₂H₃)]³⁺ has recently been shown to proceed by a reversible multistep process.^[18] To the best of our knowledge, no quantitative data on the stability of nickel urea complexes or on the kinetics of their formation in solution have been reported.



Scheme 2

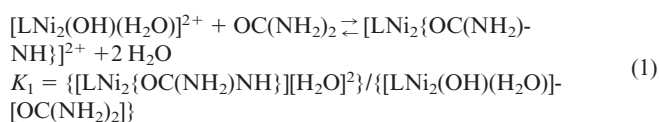
Results and Discussion

Equilibrium Studies

Initially, the behavior of **1** in various solvents and the equilibrium of urea binding (Scheme 2) were studied by UV/Vis spectroscopy.

Acetone

Complex **1** ([LNi₂(OH)(H₂O)]²⁺) has been shown to react with urea in acetone solution according to Scheme 2,^[15] with an equilibrium constant given by *K*₁ [Equation (1)].



The UV/Vis spectrum of complex **1** in acetone at 25 °C is independent of the water content in the range 0.002–0.2 M H₂O (Table 1). The species [LNi₂(OH)(H₂O)]²⁺ (**1**) ap-

Table 1. UV/Vis data of the complexes

Species	Solvent	λ_{\max}/nm ($\epsilon/\text{M}^{-1}\cdot\text{cm}^{-1}$) ^[a]
[LNi ₂ (OH)(H ₂ O)] ²⁺ (1)	acetone	405 (290), 653 (65)
1	acetonitrile (0.1 M H ₂ O)	405 (285), 653 (60)
1	methanol (2 M H ₂ O)	405 (260), 655 (60)
[LNi ₂ {OC(NH ₂)NH}] ²⁺ (2)	acetone	408 (280), 649 (65)
2	acetonitrile	408 (280), 650 (65)
2	methanol	409 (255), 652 (60)
[LNi ₂ (OH)(MeCN)] ²⁺	acetonitrile	402 (270), 647 (65)
[LNi ₂ (OH)(MeOH)] ²⁺	methanol (0.1 M H ₂ O)	409 (260), 662 (58)
[LNi ₂ (OMe)(MeOH)] ²⁺ (4)	methanol	411 (260), 675 (55)

^[a] Absorption coefficient per Ni₂ unit.

pears to be unchanged upon dissolving in such a weakly coordinating solvent as acetone, and no hydration or dehydration occurs in the solution.

Addition of urea to the solution of **1** in acetone elicits a moderate change in the UV/Vis spectrum, with the most sensitive region being 370–470 nm (Figure 1). The absorbance maximum in this region shifts from 405 to 409 nm. The change is cleanly reversed by the addition of water (Figure 2), showing that the reaction between **1** and urea is reversible. Spectrophotometric titrations performed at different concentrations of urea and water showed conserved isosbestic points (at 370 and 410 nm) and conserved extremum points in differential spectra (at 392 and 430 nm; Figure 2), suggesting that only two colored species were at equilibrium. The spectrophotometric titration data obtained in acetone at 25 °C can be fitted satisfactorily by a simple model based on Equation (1) with $K_1 = 4.3(4)$ M, confirming that urea replaces two water molecules in complex **1**.

Acetonitrile

The UV/Vis spectrum of complex **1** in acetonitrile is susceptible to the content of water. The spectrum of **1** in anhydrous acetonitrile (water content < 0.002 M) has an absorbance maximum at 402 nm and is different from that in acetone (Table 1). The addition of water systematically changes the spectrum: the absorbance maximum drifts from

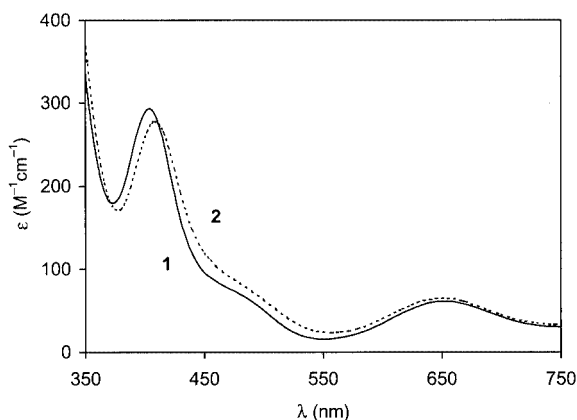


Figure 1. UV/Vis spectra of complexes **1** (solid line) and **2** (dashed line) in acetone

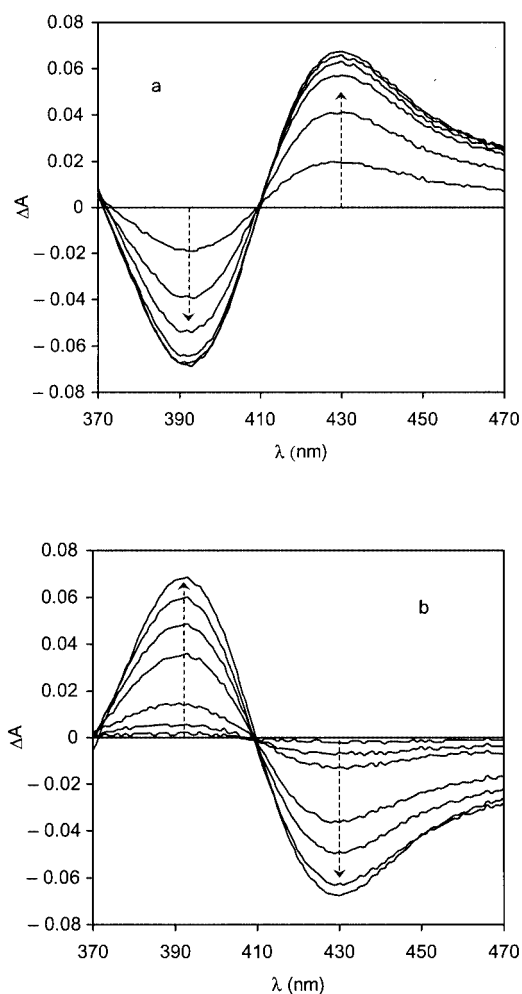
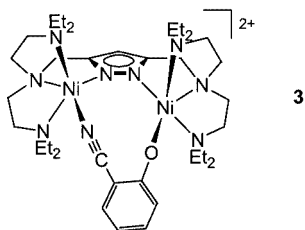
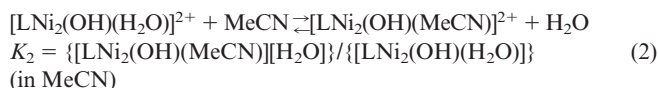


Figure 2. Differential UV/Vis spectra: (a) 2.0 mM solution of **1** in anhydrous acetone titrated with urea: 0.5, 1.0, 1.5, 2.0, 2.5, and 3.0 mM urea; (b) resulting solution titrated with water: 9, 18, 36, 112, 187, 337 mM water, the final line is for the starting complex **1**

402 to 405 nm. At $[\text{H}_2\text{O}] \geq 0.1$ M the spectrum in acetonitrile is almost congruent to that in acetone. Based on the known reactivity of complex **1** with nitriles,^[13] it can be hypothesized that acetonitrile substitutes a molecule of water to form the complex $[\text{LNi}_2(\text{OH})(\text{MeCN})]^{2+}$. Such species resemble the crystallographically characterized complex **3**.^[19]



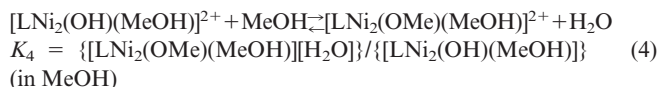
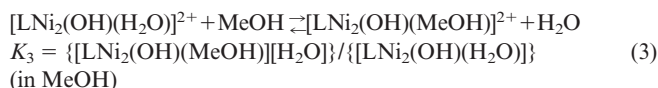
The dehydration of complex **1** in acetonitrile solution can be written as Equation (2). The equilibrium constant is estimated as $K_2 = 0.05(2)$ M. It should be noted that regular commercial acetonitrile contains about 0.1 M H_2O , in which medium the dehydration of complex **1** is insignificant.



Addition of urea to the solution of complex **1** in acetonitrile with controlled water content, $[\text{H}_2\text{O}] \geq 100$ mM, causes changes in the UV/Vis spectrum that are very similar to those observed in acetone solution (Table 1). With excess urea the spectrum is very similar to that of complex **2** in acetone. The equilibrium constant of Equation (1) in acetonitrile at 25 °C was determined as $K_1 = 2.7(5)$ M, close to that in acetone.

Methanol

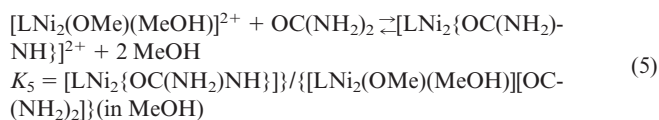
The UV/Vis spectrum of complex **1** dissolved in aqueous methanol (> 2 M H_2O) is very similar to those in acetone or aqueous acetonitrile. However, the spectrum is different in anhydrous methanol (Table 1). Spectrophotometric titration of the methanol solution of **1** with water showed two consecutive isosbestic points, suggesting that three species are at equilibrium with significantly different consecutive stability constants. As methanol and water are quite similar as ligands, it is reasonable to assume that these species are $[\text{LNi}_2(\text{OH})(\text{H}_2\text{O})]^{2+}$ (**1**), $[\text{LNi}_2(\text{OH})(\text{MeOH})]^{2+}$ and $[\text{LNi}_2(\text{OMe})(\text{MeOH})]^{2+}$ (**4**).



Indeed, the experimental data can be well fitted to the model based on Equations (3) and (4) with the consecutive equilibrium constants $K_3 = 0.040(5)$ M and $K_4 = 0.6(1)$ M at 25 °C (Scheme 3). Previous work showed that the intramolecular O_2H_3 bridging unit in type **1** complexes is rather labile, allowing for the exchange of water by other ligands,

e.g. methanol.^[13,20] Formation of complex **4** has been confirmed by its isolation and structural characterization (vide infra).

Addition of urea to the solution of complex **1** in anhydrous methanol elicits changes in the UV/Vis spectrum. The spectrum recorded for large excess of urea is very similar to that of the ureate complex **2** in other solvents (Table 1). Assuming that **4** is the dominant species in the solution of complex **1** in anhydrous methanol, the reaction can be written as Equation (5).



Data from spectrophotometric titration fit this assumption well. The equilibrium constant is $K_5 = 130(10)$ M⁻¹ at 25 °C. A combination of equilibrium constants K_3 , K_4 and K_5 allows us to calculate $K_1 = K_3K_4K_5 = 3(1)$ M in methanol at 25 °C (Scheme 3), which compares well with the values obtained in other solvents (Table 2).

Solid-State Structure of 4

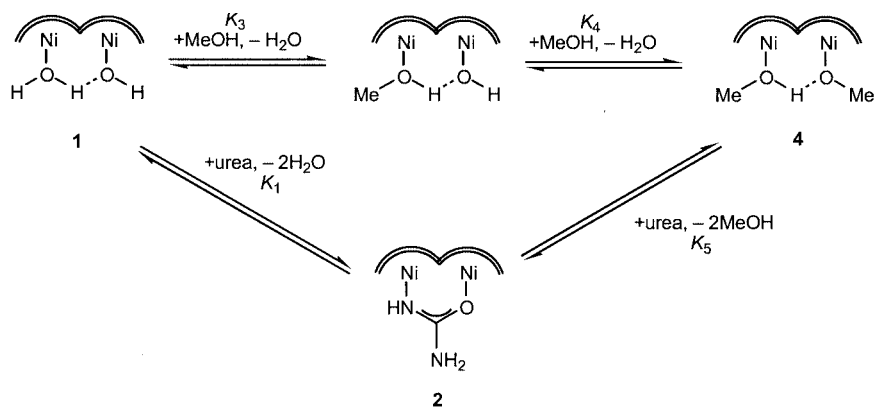
Single crystals of **4**·(ClO_4)₂ were obtained by dissolving complex **1**·(ClO_4)₂ in anhydrous methanol and subsequent slow diffusion of diethyl ether into the solution. One such crystal was analyzed by X-ray crystallography; the molecular structure of the cation is depicted in Figure 3, together with selected atom distances and bond angles.

The overall structure of **4** is very similar to that of the related O_2H_3 -bridged dinickel complex **1**·(ClO_4)₂.^[20a] As anticipated, complete exchange of water by methanol has occurred, corroborating that the intramolecular O_2H_3 bridge is labile and that binding of substrate molecules should proceed by substitution reactions within the dimetallic pocket of **1**. Both the $\text{Ni1}\cdots\text{Ni2}$ and $\text{O1}\cdots\text{O2}$ distances are slightly longer in **4** (4.552/2.426 Å in **4** versus 4.380/2.410 Å in **1**^[20a]). The coordination is very similar for both Ni1 and Ni2 and is intermediate between square-pyramidal and trigonal-bipyramidal ($\tau = 0.66$ for Ni1 and 0.62 for Ni2; the respective values for complex **1** are 0.38 and 0.82).^[21] The bridging hydrogen atom H1, located in the crystallographic analysis, was found in an asymmetric position between the two O atoms with $d(\text{O1}-\text{H1}) = 0.972$ Å and $d(\text{O2}-\text{H1}) = 1.457$ Å, but the two Ni–O bond lengths are almost identical.

The structure determination of **4** corroborates the conclusions drawn from the solution UV/Vis experiments, i.e. the O_2H_3 -bridged complex **1** is transformed into the $\text{O}_2\text{Me}_2\text{H}$ -bridged species **4** in anhydrous methanol.

Kinetic Studies

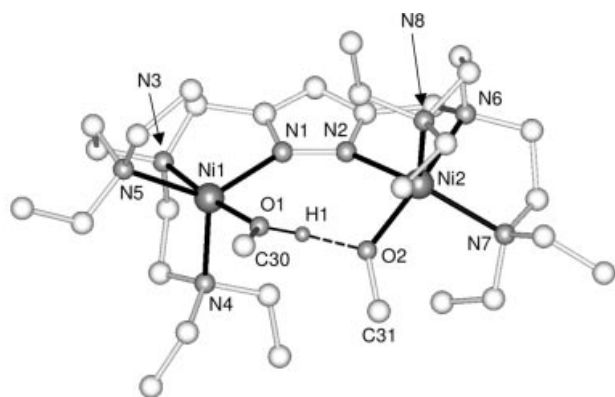
Initial kinetic experiments were performed on the exchange of methanol and water ligands in complexes $[\text{LNi}_2(\text{OR})(\text{ROH})]^{2+}$ (R = H, Me) using rapid-scanning



Scheme 3. Equilibrium processes studied

Table 2. Equilibrium constant of urea binding by complex **1** [Equation (1)] in different solvents at 25 °C

Solvent	K_1 [M]
Acetone	4.3(4)
Acetonitrile	2.7(5)
Methanol	3(1)



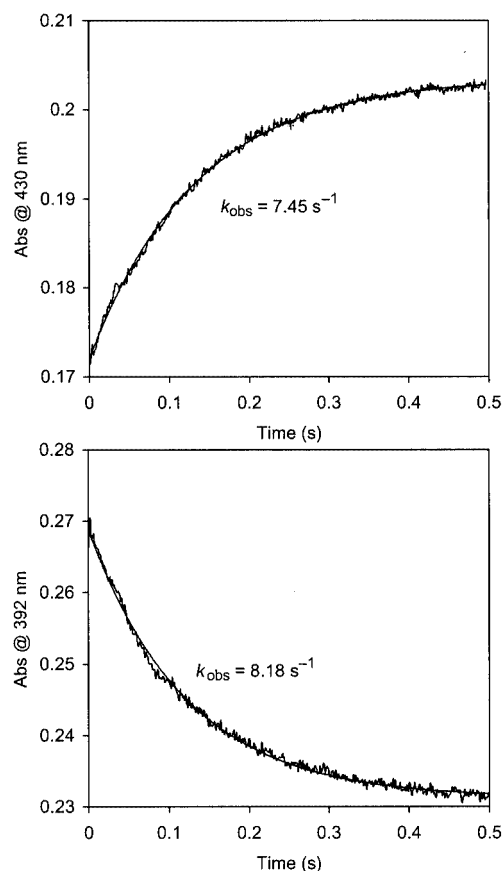


Figure 4. Representative kinetic traces of the reaction between complex **1** and urea in acetone, obtained by stopped-flow spectrophotometry, superimposed with single-exponential fits; conditions: $T = 25\text{ }^{\circ}\text{C}$, $[\mathbf{I}]_0 = 1.05\text{ mM}$, $[\text{urea}]_0 = 27.5\text{ mM}$, and $[\text{H}_2\text{O}]_0 = 10\text{ mM}$

The transformation of complex **1** into complex **2** under these conditions was not a very fast process, with k_{obs} in the range $0.3\text{--}8\text{ s}^{-1}$. The reaction is accelerated by urea

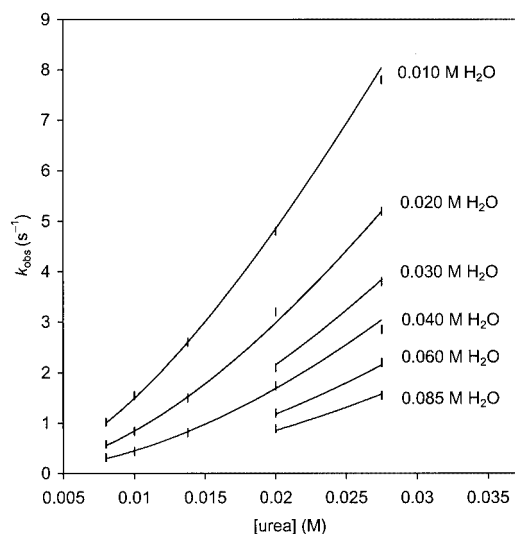


Figure 5. Pseudo first-order rate constants of the reaction between complex **1** and urea in acetone versus urea concentration in the series with constant water concentrations; lines represent the fits with Equation (6)

and decelerated by water (Figure 5). From the shapes of the concentration dependencies, k_{obs} versus $[\text{urea}]$ at constant $[\text{H}_2\text{O}]$, the reaction order in urea is evidently higher than one. Several kinetic equations were tested to fit the experimental data, and only those with both first- and second-order terms in $[\text{urea}]$ gave satisfactory fits (see Supporting Information for details; see also the footnote on the first page of this article). Equation (6) gave the best fit, and also a plausible mechanistic interpretation (*vide infra*).

$$k_{\text{obs}} = \{k'K'[\text{urea}] + k''K'K''[\text{urea}]^2\} / \{[\text{H}_2\text{O}] + K'[\text{urea}]\} \quad (6)$$

Optimization of Equation (6) by non-linear weighed least-squares method gave $k' = 0.39\text{ s}^{-1}$, $K' = 0.29$, and $k''K' = 650\text{ M}^{-1}\cdot\text{s}^{-1}$ with an average relative deviation of 2.7% and a satisfactory coverage of all experimental points (Figure 5).

Additional experiments were made to check if the reaction between **1** and urea is influenced by an external base. Addition of 2,6-dimethylpyridine (1–100 equiv.) to the solution of either complex **1** or **2** in acetone does not change the UV/Vis spectra. Also, the kinetics are constant for the reaction between complex **1** and urea in the presence of up to 10-fold excess of 2,6-dimethylpyridine versus complex **1** in acetone solution.

Methanol

As previously mentioned, complex $[\text{LNi}_2(\text{OH})(\text{H}_2\text{O})]^{2+}$ (**1**) is converted into $[\text{LNi}_2(\text{OMe})(\text{MeOH})]^{2+}$ (**4**) upon dissolution in anhydrous methanol. To minimize the interference from water, solutions of solid **4**·(ClO_4)₂ in anhydrous methanol were used. Complex **4** reacts with excess urea to yield complex **2**, as found by the equilibrium studies (*vide supra*). The formation of **2** from **4** and urea in anhydrous methanol is almost two orders of magnitude slower than from **1** and urea in anhydrous acetone at the same urea concentration. Fortunately, the solubility of urea in methanol is also much higher, allowing a wider range of

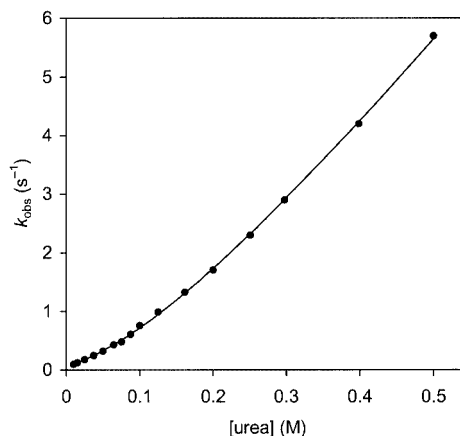


Figure 6. Pseudo first-order rate constants of the reaction between complex **4** and urea in methanol versus urea concentration ($T = 25\text{ }^{\circ}\text{C}$); experimental points superimposed with the fitting line [Equation (7)]

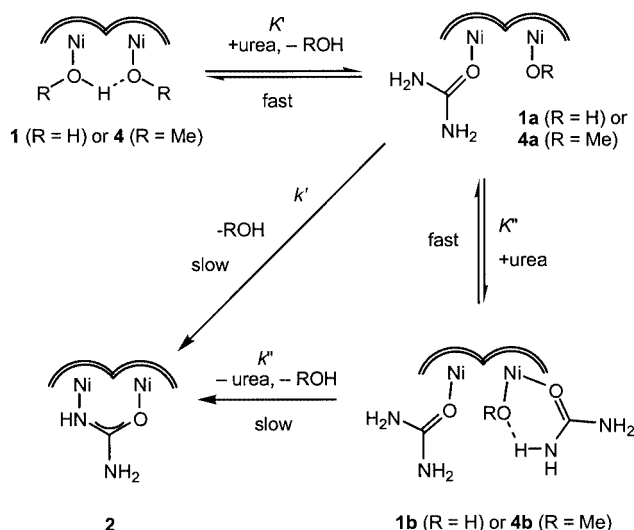
available urea concentrations. Kinetic traces of the reaction between **4** and excess urea fit perfectly with a single-exponential function in all performed experiments. The reaction accelerates with increasing in urea concentration (Figure 6). As in the reaction of **1** with urea in acetone, the kinetic data for the reaction in methanol can be fit satisfactorily only by kinetic equations with both first- and second-order terms in [urea]. Equation (7), which is very similar to Equation (6), gave the best fit for the dependence of k_{obs} versus [urea] and allowed for a similar mechanistic interpretation (vide infra).

$$k_{\text{obs}} = \{k'K'[\text{urea}] + k''K'K''[\text{urea}]^2\} / \{1 + K'[\text{urea}]\} \quad (7)$$

Optimization of Equation (7) gave $k' = 1.5 \text{ s}^{-1}$, $K' = 2.7 \text{ M}^{-1}$, and $k''K'' = 16.5 \text{ M}^{-1}\text{s}^{-1}$ with an average relative deviation of 1.1% (Figure 6).

Proposed Mechanism

As mentioned above, the experimental data for the formation of complex **2** in acetone and methanol could be fit satisfactorily only with kinetic equations having both linear and quadratic terms in urea concentration. This result strongly suggests the existence of two reactive pathways, involving one and two urea molecules, respectively. The bis(urea) pathway is dominant at all studied urea concentrations in acetone, and becomes dominant at higher urea concentrations ($> 0.08 \text{ M}$) in methanol. The bis(urea) pathway is unexpected, because only one urea molecule is incorporated into the product **2**. A mechanism shown in Scheme 4 can account for the experimental observations.



Scheme 4. Kinetic processes studied (formation of **2** was almost irreversible under the concentration conditions used)

The starting complexes **1** (in acetone) or **4** (in methanol) contain easily exchangeable solvent molecules at the LNi_2 core. Therefore, it is reasonable to assume the formation of intermediate urea complexes, $[\text{LNi}_2(\text{OR})(\text{urea})]^{2+}$ [**1a** (R = H) or **4a** (R = Me)] and $[\text{LNi}_2(\text{OR})(\text{urea})_2]^{2+}$ [**1b** (R = H)

or **4b** (R = Me)] in a fast preequilibrium with the starting complex **1** or **4**, respectively (Scheme 4). Fast exchange of monodentate ligands within the LNi_2 core has been observed for water and methanol in this work.

Steady-state mono(urea) intermediates **1a** and **4a** are formed upon the substitution of a neutral coordinated water or methanol molecule for a molecule of urea, which agrees with the kinetic Equations (6) and (7). The Ni^{II} ions in **1a** and **4a** are probably five-coordinate, as found in most complexes with the LNi_2 core and different additional ligands.^[13,19] Coordination of the neutral urea ligands in these putative intermediates is most likely *O*-monodentate, as found in most structurally characterized nickel–urea complexes.^[12,14] The equilibrium constants for the formation of **1a** and **4a** can be estimated from the kinetic data as $K'_{1a} = 0.30$ (in acetone) and $K'_{4a} = 2.7 \text{ M}^{-1}$ (in methanol). These values are reasonable, as urea is generally known to form relatively weak complexes with nickel(II) and other dipositive 3d metal cations.^[23] The substitution of a solvent molecule for urea should activate the *Ni*-bound HO^- (or MeO^- , respectively), which in **1** and **4** is present in the stabilized solvated form. The reactivity of the intermediate $[\text{LNi}_2(\text{OH})(\text{urea})]^{2+}$ ($k'_{1a} = 0.39 \text{ s}^{-1}$) is lower than that of $[\text{LNi}_2(\text{OMe})(\text{urea})]^{2+}$ ($k'_{4a} = 1.5 \text{ s}^{-1}$), in agreement with the more basic nature of the methoxide ligand. The calculated steady-state yields of intermediates **1a** and **4a** are significant (up to 40%) only at the highest used concentrations of urea, according to the kinetic data (see Supporting Information). An attempt to confirm the rapid formation of intermediate **1a** from **1** in anhydrous acetone at the high urea concentration by rapid scanning spectrophotometry was inconclusive. Upon mixing the acetone solutions of **1** and urea, the first registered spectrum (10 ms) could not be distinguished from that of the starting complex **1**. The spectral changes upon ligand substitution at the LNi_2 core are usually small, and rapid scanning gives UV/Vis spectra of relatively poor quality. Therefore, the formation of intermediates **1a** and **4a** should be considered as the most probable hypothesis.

Intermediates **1b** and **4b** are formed in solution upon binding of a second urea molecule (Scheme 4). Their yield is very small and could not be evaluated from the kinetic data. Because ligand *L* is quite bulky and usually limits the coordination number of the nickel(II) cations in the LNi_2 core to five,^[13,19] intermediates **1a** and **4a** may bind a second urea molecule only weakly (e.g., by sterically unfavorable expansion of the coordination number of a Ni^{II} cation to six, or the substitution of a diethylamino arm of ligand *L*, or hydrogen bonding). Nevertheless, the bis(urea) pathway is dominant at all studied urea concentrations in acetone and becomes dominant at $[\text{urea}] > 0.08 \text{ M}$ in methanol. Therefore, bis(urea) complexes **1b** and **4b** are much more reactive than their mono(urea) counterparts **1a** and **4a**.

A possible explanation for the unique reactivity of the putative bis(urea) intermediates is as follows. If **1b** and **4b** are formed upon *O*-coordination of two urea molecules to two different Ni^{II} centers at the LNi_2 core, then the HO^- and $\text{OC}(\text{NH}_2)_2$ ligands bound to the same Ni center may

form an intramolecular hydrogen bond as a part of six-membered pseudo-chelate cycle (Scheme 4). Such $O\cdots H-N$ bonding would make the N atom of urea more nucleophilic than in free or *O*-bound $OC(NH_2)_2$. As a consequence, an intramolecular nucleophilic attack of the urea N atom on the second Ni^{II} cation and a proton transfer from the urea to the HO^- ligand may proceed as simultaneous or closely related events, followed by the loss of water and unproductively bound urea ligands (Scheme 4). The formation of a hydrogen bond between hydroxide and urea ligands bound to different Ni atom in mono(urea) intermediates **1a** and **4a** is less probable. In this picture, the first urea molecule is required to activate the Ni-bound HO^- (or MeO^- , respectively) which in **1** and **4** is present in a stabilized solvated form, and the second urea molecule is the actual precursor of the ureate in **2**. The second urea molecule may also cause uncoordination of a diethylamino arm of the dinucleating ligand L,^[13,19] in which case the strongly basic free amino arm may play a catalytic role in the intramolecular proton transfer and the formation of the ureate anion at the LNi_2 core. Alternatively, if the second urea molecule is bound to the $[LNi_2(OR)(urea)]^{2+}$ core via hydrogen bonds it may act as a proton shuttle and facilitate the formation of the final ureate complex **2** (see Supporting Information for details).

The rate-limiting step in the formation of **2** for both mono- and bis(urea) pathways involves the bidentate *N,O*-coordination and deprotonation of an *O*-coordinated urea. The deprotonation of urea is apparently intramolecular, since Equations (1) and (5) are first-order in the dinickel complexes **1** and **4**, respectively, and the addition of an external base has no influence on the rate of Equation (1). It is not clear whether deprotonation or *N*-coordination of urea occurs first, but these events should be closely related. The amide N-atoms of neutral urea are very poor donors because of their involvement in the resonance with the carbonyl group. However, the N-atoms become very good donors upon deprotonation and the formation of an amide anion. Conversely, *N*-bound urea becomes much more acidic than *O*-bound or free urea, and its deprotonation is facilitated.^[9]

In summary, the reactive complexes **1a**, **4a**, **1b**, and **4b** with neutral urea ligands may be formed in solution in a fast preequilibrium and low yield. Formation of the final urea anion complex **2** is different. Thermodynamically, the urea anion $H_2NC(O)NH^-$ has a much higher affinity to the dinickel core than neutral urea, water, methanol, or even hydroxide or methoxide ions, because of the chelate effect and the presence of a deprotonated amide N-donor atom. Kinetically, the formation of **2** is relatively slow, because substitution of several donor atoms at the Ni^{II} centers and a proton transfer are involved. It should be noted that under the concentration conditions used in the kinetic study, the formation of the ureate complex **2** was irreversible (Scheme 4). The bridging *N,O*-coordinated urea anion at a dimetal core is quite stable and is not activated for hydrolysis.^[11,13,18] Urease avoids the deprotonation of urea at its catalytic dinickel site. In the enzyme, urea undergoes a nucleophilic attack from the hydroxide ligand, which eventu-

ally leads to hydrolysis (Scheme 1). This supports the view that nucleophilic attack and *N*-binding of the substrate have to occur simultaneously in urease. The specific action of the enzyme is probably caused by the involvement of additional groups in the stabilization of a tetrahedral intermediate and subsequent general acid/base catalysis.^[2,5] Another difference between the reactivity of urease and model complex **1** towards urea is the existence of two parallel reactive pathways for the model complex. While complexes **1** and **2** are not functional models for urease, a detailed investigation of these complexes reveals valuable insight into the binding of urea at a dinickel core.

Conclusion

The equilibrium and kinetics of urea binding by model dinickel complexes have been studied for the first time. Complexes $[LNi_2(OR)(ROH)]^{2+}$ ($R = H, Me$) with a dinucleating pyrazole-based ligand L react reversibly with urea in solution to form complex $[LNi_2[OC(NH_2)NH]]^{2+}$ with an *N,O*-bridging urea anion. Kinetic studies revealed several reaction steps in which, initially, urea substitutes the solvent molecule in $[LNi_2(OR)(ROH)]^{2+}$ to form steady-state intermediates $[LNi_2(OR)(urea)_n]^{2+}$ ($n = 1, 2$) in a fast pre-equilibrium. The subsequent bidentate *N,O*-coordination and deprotonation of an *O*-bound urea ligand constitute the rate-limiting step. Reactive complexes $[LNi_2(OH)(urea)_n]^{2+}$ are close analogs of the reactive intermediate of urease, which also has the HO^- and urea ligands bound at a dinickel core. However, the reactivities of the intermediates are different. In the urease enzyme, the HO^- ligand attacks urea as a nucleophile, leading to the hydrolysis of urea. The HO^- ligand in our model complex acts as a base towards urea, and the dinickel complex with urea anion is formed. The present study helps in understanding the factors that govern the pathway of the reaction between the HO^- and urea ligands at a dinickel core, which is a prerequisite for the design of a fully functional synthetic model of urease.

Experimental Section

Caution: Although no problems were encountered, transition metal perchlorate complexes are potentially explosive and should be handled with proper precautions!

General: Complex **1**·(ClO_4)₂ was prepared as described previously.^[13] Urea (Acros) was recrystallized three times from hot water and dried in vacuo over Drierite for 48 h before use. Anhydrous acetone (Acros), acetonitrile and methanol (Aldrich) were used as received. Solutions of the nickel complexes and urea in the anhydrous solvents were prepared and handled in a dry box. UV/Vis spectra were taken with a Hitachi U-2000 spectrophotometer at 25 °C.

Kinetic Studies: Kinetic experiments were carried out by using a Hi-Tech Scientific (Salisbury, UK) SF-43 stopped-flow apparatus with stainless steel lines. The concentrations of stock solutions were

1–4 mM $1\cdot(\text{ClO}_4)_2$ in acetone, 8–55 mM urea in acetone, 1–4 mM $4\cdot(\text{ClO}_4)_2$ in methanol, and 20–1000 mM urea in methanol. The stock solutions of a nickel complex and urea were mixed in a 1:1 ratio. Urea was always taken in at least eightfold excess to allow pseudo first-order conditions.

Urea Solubility: The solubility of urea in acetonitrile and acetone in the range of 0–30 °C was determined by gravimetric measurements. The molar solubility of urea in anhydrous acetonitrile (water content $[\text{H}_2\text{O}] \leq 0.002 \text{ M}$) is expressed by $\ln S = 6.2372 - 2615/T$; 0.079 M at 298 K. The molar solubility of urea in anhydrous acetone (water content $[\text{H}_2\text{O}] \leq 0.002 \text{ M}$) is expressed by $\ln S = 6.2628 - 2733/T$; 0.055 M at 298 K. The molar solubility of urea in regular commercial acetone (water content $[\text{H}_2\text{O}] \approx 0.2 \text{ M}$) can be satisfactorily expressed by $\ln S = 5.6253 - 2465/T$; 0.071 M at 298 K.

Synthesis of $4\cdot(\text{ClO}_4)_2$: A solution of $1\cdot(\text{ClO}_4)_2$ (0.25 g, 0.84 mmol) in anhydrous MeOH (1 mL) was layered with diethyl ether; green crystals of $4\cdot(\text{ClO}_4)_2$ gradually formed. To ensure complete replacement of water by methanol, crystallization should be carried out in the presence of predried molecular sieves. $\text{C}_{31}\text{H}_{68}\text{Cl}_2\text{N}_8\text{Ni}_2\text{O}_{10}$ (901.22): calcd. C 41.32, H 7.60, N 12.43; found C 40.40, H 7.45, N 12.41.

X-ray Crystallographic Study: Data collection for $4\cdot(\text{ClO}_4)_2$ was carried out with a Bruker AXS CCD diffractometer at 173 K by using graphite-monochromated Mo-K_α radiation ($\lambda = 0.71073 \text{ \AA}$). Structures were solved by direct methods (SHELXS-97) and refined by full-matrix least-squares techniques based on F^2 (SHELXL-97).^[24] Atomic coordinates and thermal parameters of the non-hydrogen atoms were refined in fully anisotropic models. Hydrogen atoms, except those of the disordered ethyl group, were located in difference Fourier maps and refined isotropically. One of the ethyl groups is disordered over two positions (3:1). $\text{C}_{31}\text{H}_{68}\text{Cl}_2\text{N}_8\text{Ni}_2\text{O}_{10}$, $M = 901.2$, orthorhombic, space group $Pna2_1$, $a = 25.6829(5)$, $b = 13.4179(3)$, $c = 11.9614(2) \text{ \AA}$, $V = 4122.0(2) \text{ \AA}^3$, $Z = 4$, $\rho_{\text{calcd.}} = 1.452 \text{ g cm}^{-3}$, $\mu (\text{Mo-K}_\alpha) = 1.104 \text{ mm}^{-1}$, $3.2^\circ < 2\theta < 56.7^\circ$, 40935 measured reflections, 9727 unique ($R_{\text{int}} = 0.047$), 8177 observed [$I > 2\sigma(I)$], 743 parameters, final $R1[I > 2\sigma(I)] = 0.032$, $wR2(\text{all data}) = 0.073$, goodness of fit on $F^2 = 1.049$, largest diff. peak $+0.48/-0.34 \text{ e-\AA}^{-3}$. CCDC-191806 contains the supplementary crystallographic data for this paper. These data can be obtained free of charge via www.ccdc.cam.ac.uk/conts/retrieving.html or from CCDC, 12 Union Road, Cambridge CB2 1EZ, UK [Fax: (internat.) + 44-1223/336-033; E-mail: deposit@ccdc.cam.ac.uk].

Acknowledgments

E. R. A. thanks Tufts University, the NSF, and the Research Corporation for financial support. F. M. thanks the Deutsche Forschungsgemeinschaft and the Fonds der Chemischen Industrie for financial support.

- [1] [1a] N. E. Dixon, C. Gazzola, R. L. Blakeley, B. Zerner, *J. Am. Chem. Soc.* **1975**, *97*, 4131–4133. [1b] M. A. Halcrow, G. Christou, *Chem. Rev.* **1994**, *94*, 2421–2481. [1c] S. Lippard, *Science* **1995**, *268*, 996–997. [1d] J. C. Fontecilla-Camps, *Struct. Bonding* **1998**, *91*, 1–30. [1e] M. J. Maroney, G. Davidson, C. B. Allan, J. Figlar, *Struct. Bonding* **1998**, *92*, 1–64.
- [2] P. A. Karplus, M. A. Pearson, R. P. Hausinger, *Acc. Chem. Res.* **1997**, *30*, 330–337.
- [3] R. L. Blakeley, A. Treston, R. K. Andrews, B. Zerner, *J. Am. Chem. Soc.* **1982**, *104*, 612–614.

- [4] E. Jabri, M. B. Carr, R. P. Hausinger, P. A. Karplus, *Science* **1995**, *268*, 998–1003.
- [5] [5a] E. Jabri, P. A. Karplus, *Biochemistry* **1996**, *35*, 10616–10626. [5b] I.-S. Park, L. O. Michel, M. A. Pearson, E. Jabri, P. A. Karplus, S. Wang, J. Dong, R. A. Scott, P. B. Köhler, M. K. Johnson, R. P. Hausinger, *J. Biol. Chem.* **1996**, *271*, 18632. [5c] M. A. Pearson, L. O. Michel, R. P. Hausinger, P. A. Karplus, *Biochemistry* **1997**, *36*, 8164–8172. [5d] S. Benini, W. R. Rypniewski, K. S. Wilson, S. Ciurli, S. Mangani, *J. Biol. Inorg. Chem.* **1998**, *3*, 268–273. [5e] S. Benini, W. R. Rypniewski, K. S. Wilson, S. Miletto, S. Ciurli, S. Mangani, *J. Biol. Inorg. Chem.* **2000**, *5*, 110–118. [5f] M. A. Pearson, I.-S. Park, R. A. Schaller, L. O. Michel, P. A. Karplus, R. P. Hausinger, *Biochemistry* **2000**, *39*, 8575–8584. [5g] N.-C. Ha, S.-T. Oh, J. Y. Sung, K. A. Cha, M. H. Lee, B.-H. Oh, *Nature Struct. Biol.* **2001**, *8*, 505–509.
- [6] S. Ciurli, S. Benini, W. R. Rypniewski, K. S. Wilson, S. Miletto, S. Mangani, *Coord. Chem. Rev.* **1999**, *190–192*, 331–355.
- [7] S. Benini, W. R. Rypniewski, K. S. Wilson, S. Miletto, S. Ciurli, S. Mangani, *Structure* **1999**, *7*, 205–216. [7a] S. Benini, W. R. Rypniewski, K. S. Wilson, S. Miletto, S. Ciurli, *J. Biol. Inorg. Chem.* **2001**, *6*, 778–790.
- [8] [8a] F. Musiani, S. Arnoffi, R. Casadio, S. Ciurli, *J. Biol. Inorg. Chem.* **2001**, *6*, 300–314. [8b] M. J. Todd, R. P. Hausinger, *Biochemistry* **2000**, *39*, 5389–5396.
- [9] T. C. Woon, W. A. Wickramasinghe, D. P. Fairlie, *Inorg. Chem.* **1993**, *32*, 2190–2194.
- [10] N. E. Dixon, P. W. Riddles, C. Gazzola, R. L. Blakeley, B. Zerner, *Can. J. Biochem.* **1980**, *58*, 1335–1344.
- [11] S. Buchler, F. Meyer, E. Kaifer, H. Pritzkow, *Inorg. Chim. Acta* **2002**, *337*, 371–386.
- [12] [12a] R. M. Buchanan, M. S. Mashuta, K. J. Oberhausen, J. F. Richardson, *J. Am. Chem. Soc.* **1989**, *111*, 4497–4498. [12b] A. J. Stemmler, J. W. Kampf, M. L. Kirk, V. L. Pecoraro, *J. Am. Chem. Soc.* **1995**, *117*, 6368–6369. [12c] D. Volkmer, A. Hörstmann, K. Griesar, W. Haase, B. Krebs, *Inorg. Chem.* **1996**, *35*, 1132–1135. [12d] D. Volkmer, B. Hommerich, K. Griesar, W. Haase, B. Krebs, *Inorg. Chem.* **1996**, *35*, 3792–3803. [12e] F. Meyer, A. Jacobi, B. Nuber, P. Rutsch, L. Zsolnai, *Inorg. Chem.* **1998**, *37*, 1213–1218. [12f] Hosokawa, H. Yamane, Y. Nakao, K. Matsumoto, S. Takamizawa, W. Mori, S. Suzuki, H. Kimoto, *Inorg. Chim. Acta* **1998**, *283*, 118–123. [12g] D. A. Brown, L. P. Cuffe, O. Deeg, W. Errington, N. J. Fitzpatrick, W. K. Glass, K. Herlihy, T. J. Kemp, H. Nimir, *Chem. Commun.* **1998**, 2433–2434. [12h] M. Arnold, D. A. Brown, O. Deeg, W. Errington, W. Haase, K. Herlihy, T. J. Kemp, H. Nimir, R. Werner, *Inorg. Chem.* **1998**, *37*, 2920–2925. [12i] S. Uozumi, H. Furutachi, M. Ohba, H. Okawa, D. E. Fenton, K. Shindo, S. Murata, D. J. Kitko, *Inorg. Chem.* **1998**, *37*, 6281–6287. [12j] B. Hommerich, H. Schwöppe, D. Volkmer, B. Krebs, *Z. Anorg. Allg. Chem.* **1999**, *625*, 75–82. [12k] A. M. Barrios, S. J. Lippard, *J. Am. Chem. Soc.* **1999**, *121*, 11751–11757. [12l] H. Carlsson, M. Haukka, E. Nordlander, *Inorg. Chem.* **2002**, *41*, 4981–4983.
- [13] F. Meyer, E. Kaifer, P. Kircher, K. Heinze, H. Pritzkow, *Chem.-Eur. J.* **1999**, *5*, 1617–1630.
- [14] [14a] H. E. Wages, K. L. Taft, S. J. Lippard, *Inorg. Chem.* **1993**, *32*, 4985–4987. [14b] K. Yamaguchi, S. Koshino, F. Akagi, M. Suzuki, A. Uehara, S. Suzuki, *J. Am. Chem. Soc.* **1997**, *119*, 5752–5753. [14c] T. Koga, H. Furutachi, T. Nakamura, N. Fukita, M. Ohba, K. Takahashi, H. Okawa, *Inorg. Chem.* **1998**, *37*, 989–996. [14d] M. Konrad, F. Meyer, A. Jacobi, P. Kircher, P. Rutsch, L. Zsolnai, *Inorg. Chem.* **1999**, *38*, 4559–4566. [14e] A. M. Barrios, S. J. Lippard, *J. Am. Chem. Soc.* **2000**, *122*, 9172–9177. [14f] A. M. Barrios, S. J. Lippard, *Inorg. Chem.* **2001**, *40*, 1060–1064.
- [15] F. Meyer, H. Pritzkow, *Chem. Commun.* **1998**, 1555–1556.
- [16] F. Meyer, M. Konrad, E. Kaifer, *Eur. J. Inorg. Chem.* **1999**, 1851–1854.
- [17] F. Meyer, P. Rutsch, *Chem. Commun.* **1998**, 1037–1038.

- [18] S. V. Kryatov, A. Y. Nazarenko, P. D. Robinson, E. V. Rybak-Akimova, *Chem. Commun.* **2000**, 921–922.
- [19] F. Meyer, I. Hyla-Kryspin, E. Kaifer, P. Kircher, *Eur. J. Inorg. Chem.* **2000**, 771–781.
- [20] [20a] L. Siegfried, T. A. Kaden, F. Meyer, P. Kircher, H. Pritzkow, *J. Chem. Soc., Dalton Trans.* **2001**, 2310–2315. [20b] J. Ackermann, F. Meyer, E. Kaifer, H. Pritzkow, *Chem.-Eur. J.* **2002**, 8, 247–258.
- [21] The angular structural parameter τ is defined as $\tau = (\beta - \alpha)/60$, where α and β represent two basal angles with $\beta > \alpha$. It is a measure for the degree of trigonality: a perfect TB-5 structure is associated with $\tau = 1$, while $\tau = 0$ is expected for an idealized SPY-5 geometry: A. W. Addison, T. N. Rao, J. Reedijk, J. van Rijn, G. C. Verschoor, *J. Chem. Soc., Dalton Trans.* **1984**, 1349–1356.
- [22] A. E. Merbach, *Pure Appl. Chem.* **1982**, 54, 1479–1493.
- [23] [23a] A. F. Borina, V. T. Orlova, S. A. Popova, *Zh. Neorg. Khim.* **1991**, 36, 2617–2622. [23b] V. A. Prokuev, V. V. Zapyshnyi, *Zh. Neorg. Khim.* **1998**, 43, 810–814.
- [24] G. M. Sheldrick, *SHELXS-97, Program for Crystal Structure Solution*, Universität Göttingen, **1997**; G. M. Sheldrick, *SHELXL-97, Program for Crystal Structure Refinement*, Universität Göttingen, **1997**.

Received October 23, 2002
[I02584]